Supporting Information

Green synthesis of mesoporous $MnNbO_x$ oxide by liquid induced self-assembly strategy for low-temperature removal of NO_x

Huifang Cheng[a,†], Guodong Feng[b,c,d,†], Zhenzhen Yang[c], Tao Wang[c], Francis Okejiri[c], Junbin Tan[b], Minjie Zhao[b], Jixing Liu[b,c]*, Jian Liu[b,]*, Zhen Zhao[b]

[a]College of Material Science and Engineering, Hebei University of Engineering, Handan 056038, Hebei, People's Republic of China;

[b]State Key Laboratory of Heavy Oil and Beijing Key Lab of Oil & Gas Pollution Control, China University of Petroleum, Beijing 102249, P. R. China;

[c]Department of Chemistry, University of Tennessee-Knoxville, Tennessee 37996-1600, United States;

[d]Key Laboratory of Advanced Molecular Engineering Materials, College of Chemistry and Chemical Engineering, Baoji University of Arts and Sciences, Baoji 721013, P. R. China;

*Corresponding authors: J.X.L. (E-mail: jxliu0804@gmail.com) and J.L. (E-mail: liujian@cup.edu.cn)

Experimental section

1.1. Synthesis of Catalysts. In a typical synthesis of mesoporous $MnNbO_x$ oxide, 0.65 g of niobium (V) ethoxide (99.999%, Alfa), 2.0 g $Mn(OOCCH_3)_2{\cdot}4H_2O$ (99%, Aldrich) and 1.0 g of ionic liquid ($BmimTf_2N$) were dissolved in 5.0 ml of ethanol. The solution was stirred at room temperature for 2 h until $Mn(OOCCH_3)_2{\cdot}4H_2O$ was completely dissolved. Subsequently, ethanol (5.0 ml) was added slowly with stirring. The mixed solution was gelled in an open petridish at 50 ^oC for 24 h and aged at 200 ^oC for 2 h, and a solid film was obtained. The ionic liquid was extracted by refluxing the sample with ethanol in a Soxhlet extractor for 24 h. The as-made sample was thermally treated at 550 ^oC for 2 h with the heating rate of $1K{\cdot}min^{-1}$ in air, and the final sample denoted as meso-$MnNbO_x$.

For comparison purpose, the counterpart catalyst with the same composition as porous meso-$MnNbO_x$ was synthesized by a co-precipitation method.

1.2. Catalysts characterization. The microstructure of $MnNbO_x$ catalysts was conducted on a JEOL JEM LaB6 2100 electron microscope. The phase composition and texture properties of various $MnNbO_x$ oxides were detected by the XRD and N_2 adsorption-desorption isotherm performed on Micromeritics Tristar Ⅱ 3020 porosimetry analyzer at −196 ^oC. The microstructure and the particle size of the $MnNbO_x$ catalysts were observed by FEI QUANTA 430 thermal field emission scanning electron microscope (SEM). Surface chemical valence states of $MnNbO_x$ oxides were investigated by X-ray photoelectron spectra (XPS) carried out on a PerkinElmer PHI-1600 ESCA spectrometer using Al Kα anode ($h\nu$ = 1253.6 eV) as X-ray source. The element content of as-prepared materials was determined by a Varian 715-ES inductively coupled plasma-atomic emission spectrometer (ICP-AES). Hydrogen (H_2) temperature-programmed reduction (H_2-TPR) measurements were performed on a USA Autosorb-iQ-C chemisorption analyzer (Quantachrome). Ammonia temperature-programmed desorption (NH_3-TPD) experiments were conducted on a USA Quantachrome apparatus. The adsorption properties of NH_3 and NO_x were probed by *in-situ* diffuse reflection fourier transform infrared spectroscopy (DRIFTS) on a Nicolet IS50 FT-IR spectrometer.

1.3. NH_3-SCR of NO_x test. NH_3-SCR of NO_x evaluations for $MnNbO_x$ catalysts were carried out on a micro instrument under atmospheric pressure. Prior to the measurement of NO_x light-off curves, 0.20 g catalyst protected by quartz wool was placed into the reactor. Thereafter, the feed gas ($500\ ml{\cdot}min^{-1}$) consisted of 100 ppm SO_2 (when used), 5% H_2O (when used), 3% O_2, 500 ppm NH_3, 500 ppm NO balanced with N_2 were injected into the fixed-bed reactor and corresponding gas hourly space velocity (GHSV) of 100,000 h^{-1}. The feed gas concentrations were determined by the NO_x analyzer (SIGNAL4000 120 VM), and the composition of feed gases at

the outlet was measured by Thermo Nicolet iS-50 spectrometer. Finally, NO_x conversion and N_2 selectivity were calculated based on the following equations:

$$NO_x \text{ conversion} = \frac{[NO_x]_{inlet} - [NO_x]_{outlet}}{[NO_x]_{inlet}} \times 100\% \quad (1)$$

$$N_2 \text{ Selectivity} = \left(1 - \frac{2[N_2O]_{outlet}}{[NO_x]_{inlet} + [NH_3]_{inlet} - [NO_x]_{outlet} - [NH_3]_{outet}}\right) \times 100\% \quad (2)$$

Table S1 Textural properties of $MnNbO_x$ catalysts.

Sample	S_{BET} (m^2/g)	V (cm^3/g)	D (nm)	Integrated total TPD yields [a]	Concentration (wt.%) [b]	
					Mn	Nb
meso-$MnNbO_x$	116.0	0.37	13.7	1694.2	56.4	14.1
bulk-$MnNbO_x$	29.9	0.10	16.2	757.7	54.3	16.2

[a] Obtained by TPD.

[b] Obtained by ICP.

Table S2 The surface atomic concentrations of Mn, Nb, O, and the relative concentration ratios.

Catalyst	surface atomic concentrations			relative concentration ratios								
	Mn	Nb	O	Mn^{2+}	Mn^{3+}	Mn^{4+}	R^a	Nb^{4+}	Nb^{5+}	R^b	O_α	O_β
meso-$MnNbO_x$	0.21	0.6	0.73	0.17	0.62	0.21	2.95	0.22	0.78	0.28	0.69	0.31
bulk-$MnNbO_x$	0.20	0.08	0.72	0.28	0.43	0.29	1.48	0.33	0.67	0.49	0.66	0.34

[a] The Ce species ratio of Mn^{3+}/Mn^{4+};
[b] The O species ratio of Nb^{4+}/Nb^{5+}.

Table S3 Comparison of NH_3-SCR performance over meso-$MnNbO_x$ with the state-of-the-art catalysts and other mesoporous oxides prepared with soft- or hard-templating methods.

Catalyst	Reaction Condition	C (T/°C)	Temperature Window (°C)	Reference
meso-$MnNbO_x$	[NO] = [NH_3] = 500 ppm, [O_2] = 3 vol.%, GHSV = 100,000 h^{-1}	100% (100)	100−225	This work
Fe/TiO_2	[NO] = [NH_3] = 200 ppm, [O_2] = 5 vol.%, GHSV = 12,000 h^{-1}	100% (230)	230−275	1
Mn/TiO_2	[NO] = [NH_3] = 1000 ppm, [O_2] = 3 vol.%, GHSV = 30,000 h^{-1}	100% (110)	—	2
MnO_2	[NO] = [NH_3] = 500 ppm, [O_2] = 5 vol.%, GHSV = 50,000 h^{-1}	98% (160)	160−220	3
MnO_x-CeO_2/SBA-15	[NO] = 1000 ppm, [NH_3] = 1100 ppm, [O_2] = 8 vol.%, GHSV = 10,000 h^{-1}	90% (150)	150−275	4
MnO_x-CeO_2	[NO] = [NH_3] = 300 ppm, [O_2] = 5 vol.%, GHSV = 120,000 h^{-1}	90% (150)	150−240	5
meso-$NiMnO_x$	[NO] = [NH_3] = 500 ppm, [O_2] = 5 vol.%, GHSV = 60,000 h^{-1}	100% (150)	150−275	6
CuO/MnO_2-mTiO_2	[NO] = [NH_3] = 1000 ppm, [O_2] = 5 vol.%, GHSV = 20,000 h^{-1}	98% (160)	160−280	7
$FeMnZrO_x$	[NO] = [NH_3] = 500 ppm, [O_2] = 4 vol.%, GHSV = 35,000 h^{-1}	100% (200)	200−360	8
Sn/Cr-MnO_x	[NO] = [NH_3] = 500 ppm, [O_2] = 3 vol.%, GHSV = 35,000 h^{-1}	100% (150)	150−250	9
meso-$MnCo_2O_4$	[NO] = [NH_3] = 500 ppm, [O_2] = 3 vol.%, GHSV = 32,000 h^{-1}	95% (100)	100−250	10
WO_3(1)-CeO_2	[NO] = [NH_3] = 500 ppm, [O_2] = 5 vol.%, GHSV = 30,000 h^{-1}	100% (225)	225−350	11
$CeWO_x$	[NO] = [NH_3] = 500 ppm, [O_2] = 5 vol.%, GHSV = 300,000 h^{-1}	90% (250)	250−425	12

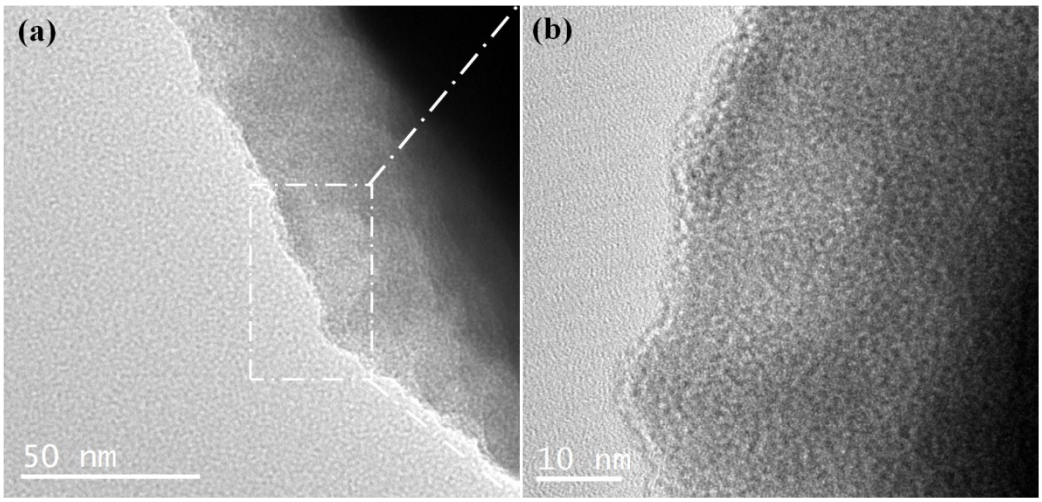

Fig. S1 (a) TEM image and (b) HRTEM image of metal salt/ionic liquid precursor.

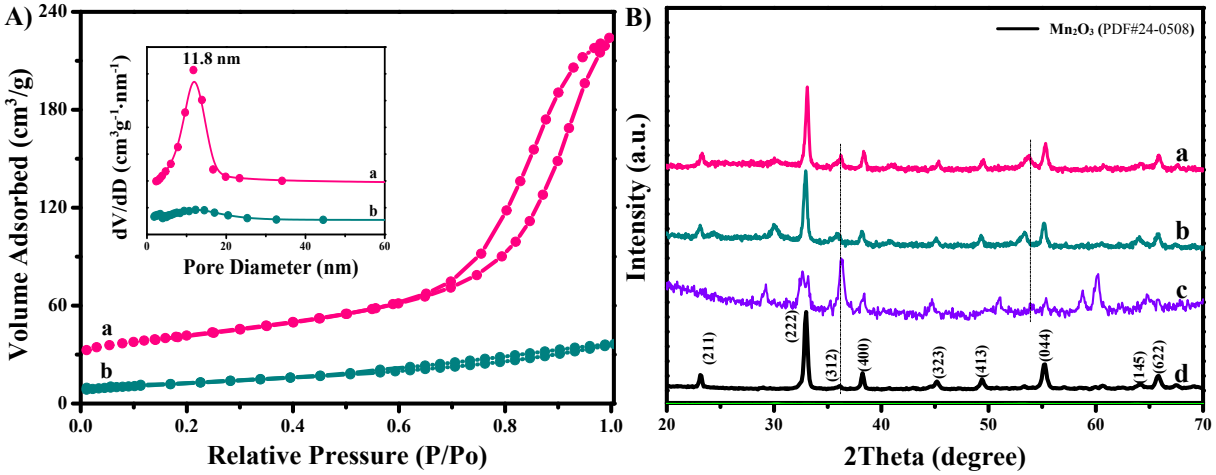

Fig. S2 (A) Nitrogen adsorption-desorption isotherms and size distribution curves, and (B) XRD profile of the catalysts: (a) meso-$MnNbO_x$, (b) bulk-$MnNbO_x$ (c) NbO_x, and (d) Mn_2O_3.

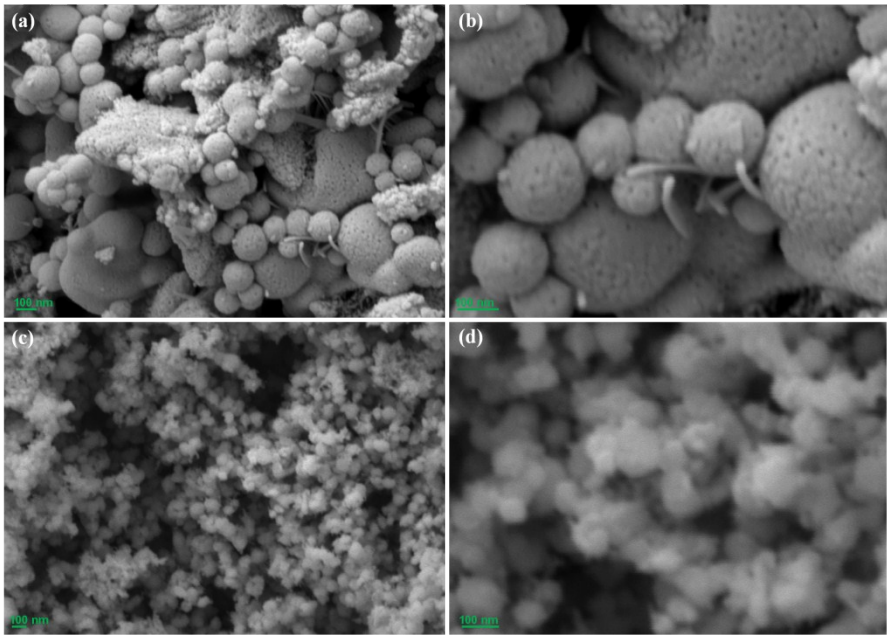

Fig. S3 SEM images of the catalysts: (a)meso-$MnNbO_x$ and (b) bulk-$MnNbO_x$.

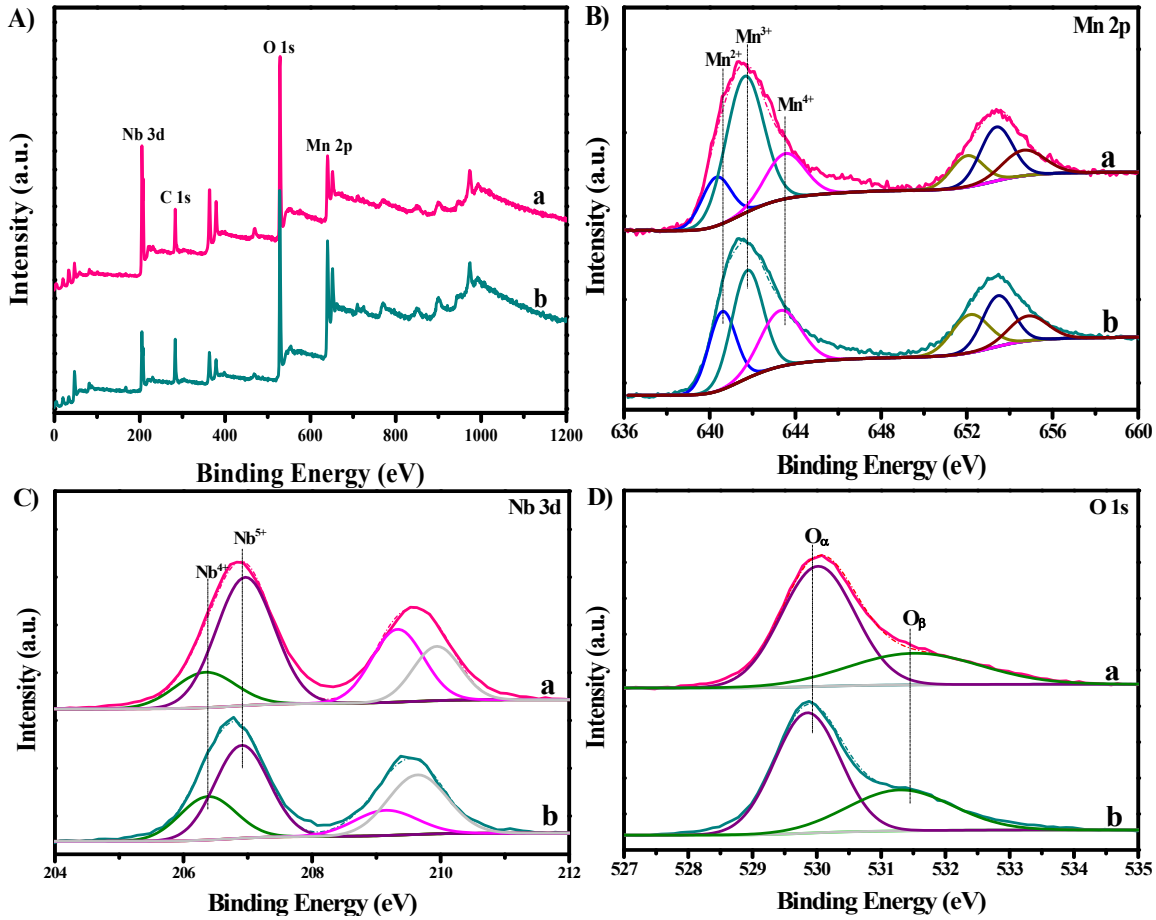

Fig. S4 (A) XPS full spectra, (B) Mn 2p, (C) Nb 3d, and (D) O 1s of the catalysts: (a) meso-$MnNbO_x$ and (b) bulk-$MnNbO_x$.

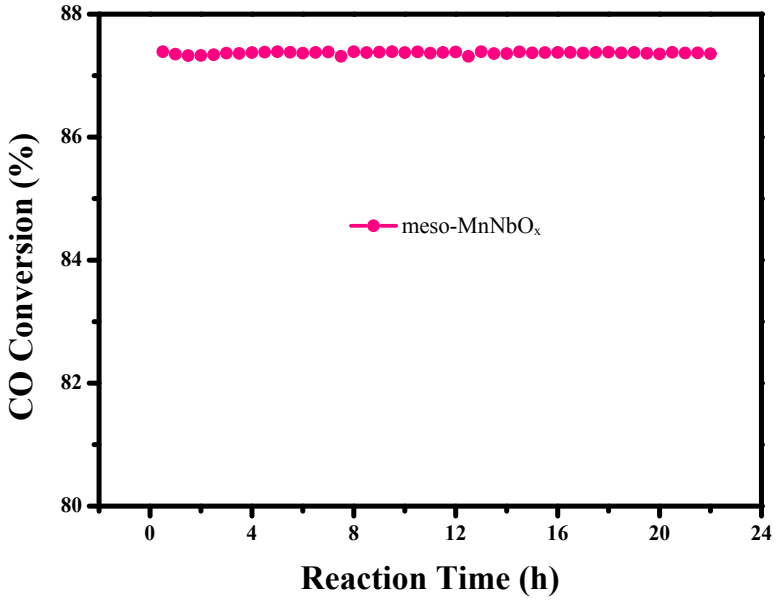

Fig. S5 Stability test of meso-$MnNbO_x$ catalyst at 280 °C. Reaction conditions: [NO] = [NH_3] = 500 ppm, [O_2] = 3 vol.%, balanced with N_2, GHSV = 100,000 h^{-1}.

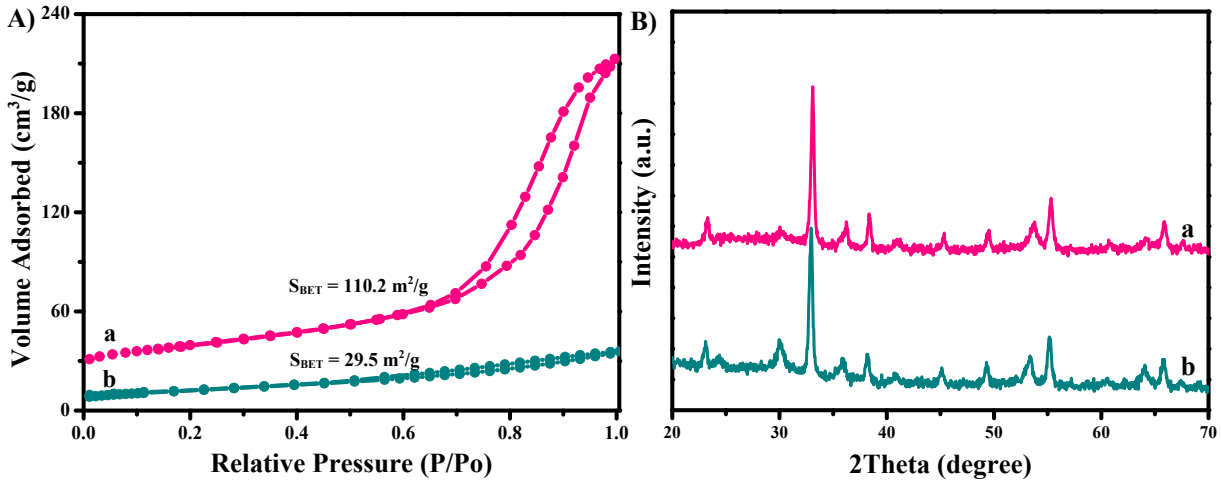

Fig. S6 (A) Nitrogen adsorption-desorption isotherms, and (B) XRD profile of the recovered catalysts after stability test: (a) meso-$MnNbO_x$ and (b) bulk-$MnNbO_x$.

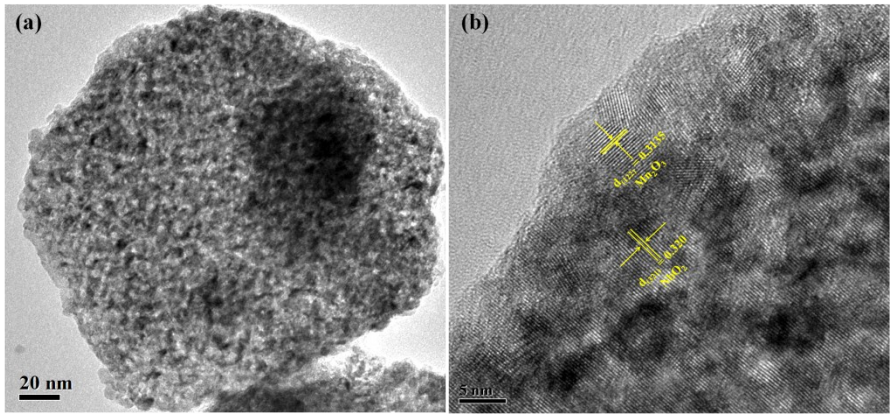

Fig. S7 (a) TEM image and (b) HRTEM images of the recovered meso-$MnNbO_x$ catalyst after stability test.

References

1. Y. Li, X. Han, Y. Hou, Y. Guo, Y. Liu, N. Xiang, Y. Cui and Z. Huang, *Chinese J. Catal.*, 2017, **38**, 1831-1841.
2. Y. Shi, S. Chen, H. Sun, Y. Shu and X. Quan, *Catal. Commun.*, 2013, **42**, 10-13.
3. H. Jiang, Y. Wang, J. Zhou, Y. Chen and M. Zhang, *Mater. Lett.*, 2018, **233**, 250-253.
4. X. Ran, M. Li, K. Wang, X. Qian, J. Fan, Y. Sun, W. Luo, W. Teng, W.-x. Zhang and J. Yang, *ACS Appl. Mater. Interfaces*, 2019, **11**, 19242-19251.
5. Y. Yue, Y. Wang, J. Ling, W. Sun and Z. Shen, *Aust. J. Chem.*, 2019, **72**, 657-662.
6. H. Zhang, H. Wang, Z. Hao, R. Wang, Y. Xia, P. Wang and S. Zhan, *Acs Applied Nano Materials*, 2019, **2**, 505-516.
7. J. Fan, M. Lv, W. Luo, X. Ran, Y. Deng, W.-x. Zhang and J. Yang, *Chem. Commun.*, 2018, **54**, 3783-3786.
8. N. Fang, J. Guo, S. Shu, H. Luo, Y. Chu and J. Li, *Chem. Eng. J.* 2017, **325**, 114-123.
9. M. Qiu, S. Zhan, D. Zhu, H. Yu and Q. Shi, *Catal. Today*, 2015, **258**, 103-111.
10. M. Qiu, S. Zhan, H. Yu, D. Zhu and S. Wang, *Nanoscale*, 2015, **7**, 2568-2577.
11. S. Zhan, H. Zhang, Y. Zhang, Q. Shi, Y. Li and X. Li, *Applied catalysis. B, Environmental*, 2017, **203**, 199-209.
12. W. Shan, Y. Geng, X. Chen, N. Huang, F. Liu and S. Yang, *Catal. Sci. Technol.*, 2016, **6**, 1195-1200.